

---

---

ELECTRICAL AND MAGNETIC  
PROPERTIES

---

---

## Interrelation of Hysteresis Characteristics of a Soft Magnetic Nanocrystalline Alloy

Yu. N. Starodubtsev<sup>a, b</sup>, V. A. Kataev<sup>a, \*</sup>, K. O. Bessonova<sup>a</sup>, and V. S. Tsepelev<sup>a</sup>

<sup>a</sup>Ural Federal University Named after the First President of Russia B.N. Yeltsin, Ekaterinburg, 620002 Russia

<sup>b</sup>Scientific Production Association Gammamet, Ekaterinburg, 620028 Russia

\*e-mail: vakataev@urfu.ru

Received April 26, 2018; revised July 16, 2018

**Abstract**—The relationships which interconnect parameters of static magnetic hysteresis loops, namely, hysteresis losses, coercive force, and remanence, have been obtained. These relationships arise from the similarity of dimensionless hysteresis quantities in the magnetic field range corresponding to the increase in the magnetic permeability. An experimental check was performed using the soft magnetic nanocrystalline Fe<sub>72.5</sub>Cu<sub>1</sub>Nb<sub>2</sub>Mo<sub>1.5</sub>Si<sub>14</sub>B<sub>9</sub> alloy. It was shown that, at given values of magnetic induction  $B_{\max}$  and magnetic field  $H_{\max}$ , the required hysteresis quantity can be calculated using experimental values of the other hysteretic quantities.

**Keywords** dimensional hysteresis quantity, hysteresis losses, coercive force, remanence, soft magnetic nanocrystalline alloy

**DOI:** 10.1134/S0031918X19020170

### INTRODUCTION

The magnetic hysteresis phenomenon plays a significant part in ferromagnetic materials applied in energy delivery and conversion devices [1, 2]. The magnetic hysteresis is seen in lagging the magnetic induction  $B$  (or magnetization  $M$ ) from the external magnetic field  $H$  [3]. The ambiguous dependence  $B = f(H)$  upon cyclic changes of the magnetic field is the continuous closed hysteresis loops. The limiting values of the loop are the maximum magnetic field strength  $H_{\max}$  and maximum magnetic induction  $B_{\max}$ . The points of intersection of the loop with coordinate axes (the coercive force  $H_c$  and remanence  $B_r$ ) and the area under the hysteresis curve (hysteretic losses  $W_h$ ) characterize the hysteresis properties of material and are referred to as hysteresis quantities.

Investigating the dependence of hysteresis quantities on the intensity of external action allows us to obtain new information about the nature of magnetic hysteresis. The intensity of external action is characterized by the magnetic field strength  $H_{\max}$ . The magnetic induction is the response of a substance to the external action, and the  $B_{\max}$  value also indicates the effect of magnetic hysteresis. C. P. Steinmetz [4] was the first to obtain the dependence of hysteretic losses on the magnetic induction in the form of the power function  $W_h = rB_{\max}^s$ . It was found in [4] that, for iron in the range of operating induction, the power is  $s = 1.6$ . Subsequently, the approximation of hysteresis

quantities with the power function  $Y = rX^s$  was usually used in studying magnetic hysteresis [5–8]. Such a property of the power function as its scale invariance favors the wide use of the function. Indeed, the change of independent variable by scale factor  $k$  leads only to the change in the function scale by  $k^s$  times:  $Y(kX) = r(kX)^s = rk^s X^s$ . Therefore, all power functions with the same power index  $s$  are equivalent to each other and differ only in the scale, whereas the change in the power index value  $s$  involves the qualitative change in the behavior of functional dependence. Hence, using changes in the power index in the Steinmetz's equation, it is possible to judge on the appearance of qualitative changes in the magnetization reversal process of a ferromagnetic material.

The hysteresis quantities, namely, the coercive force, remanence, and hysteretic losses are the characteristics of the same phenomenon. Due to this, the hysteresis quantities are not independent and should be interrelated. Showing the interrelation of hysteresis quantities for different magnetic materials was one of the aims of studies [9–13]. However, substantiated relationships between the hysteresis quantities have not been obtained yet. In the present study, the interrelation of quantities characterizing the magnetic hysteresis loops of the soft magnetic nanocrystalline Fe<sub>72.5</sub>Cu<sub>1</sub>Nb<sub>2</sub>Mo<sub>1.5</sub>Si<sub>14</sub>B<sub>9</sub> is studied using the similitude method of dimensionless quantities of hysteresis loops [14, 15].

## EXPERIMENTAL

The soft magnetic  $\text{Fe}_{72.5}\text{Cu}_1\text{Nb}_2\text{Mo}_{1.5}\text{Si}_{14}\text{B}_9$  alloy was melted using an induction furnace. A ribbon 25  $\mu\text{m}$  thick and 10 mm wide with the amorphous structure was prepared by planar-flow melt quenching. The ribbon was used to wind up toroidal samples 32 mm in outer diameter and 20 mm in internal diameter. To form the nanocrystalline state, the samples were subjected to heat treatment at 823 K for 1 h. The parameters of static magnetic hysteresis loop were measured using a MMKC-100-05 computer-controlled measuring system. Before measuring each loop, the sample was demagnetized using damped ac magnetic field. The computer-controlled measuring system ensures the following errors of determination of magnetic characteristics: 2% for the magnetic field strength, 5% for the hysteretic losses, and 3% for the magnetic induction, coercive force, and remanence. The ultimate error of calculation of hysteresis characteristics using the measured values did not exceed 8%.

## RESULTS AND DISCUSSION

In [14, 15], by using Rayleigh equations, the dimensionless hysteresis quantities were obtained:

$$\frac{B_r}{B_{\max}} = \frac{1}{2(\kappa_r + 1)}; \quad (1)$$

$$\frac{H_c}{H_{\max}} = \frac{F}{2(\kappa_r + 1)}; \quad (2)$$

$$\frac{W_h}{W_{\max}} = \frac{4}{3(\kappa_r + 1)}. \quad (3)$$

Here, the quantity  $W_{\max}$  equal to the product of the maximum magnetic induction and maximum magnetic field

$$W_{\max} = B_{\max}H_{\max}, \quad (4)$$

is the maximum potential energy of magnetic field per unit volume. The hysteresis factor  $\kappa_r$  is

$$\kappa_r = \frac{\mu_i}{\eta H_{\max}}, \quad (5)$$

where  $\mu_i$  is the initial magnetic permeability and  $\eta$  is the Rayleigh constant, which characterizes the relation of reversible and irreversible magnetization reversal processes. When  $\kappa_r > 1$ , the initial permeability  $\mu_i$  makes the maximum contribution to the value of  $\mu$  magnetic permeability considering that

$$\mu = \frac{B_{\max}}{\mu_0 H_{\max}} = \mu_i + \eta H_{\max}. \quad (6)$$

The dimensionless hysteresis function

$$F = 2(\kappa_r + 1) \left[ -(\kappa_r + 1) + \sqrt{(\kappa_r + 1)^2 + 1} \right] \quad (7)$$

approximately is equal to unity in the Rayleigh range, for which  $\kappa_r > 1$ . For  $\kappa_r = 25, 10, 5$ , and  $1$ ,  $F = 1.000, 0.998, 0.993$ , and  $0.944$ , respectively. Thus, in the Rayleigh range, the relative hysteresis quantities (1)–(3) have similar dependences on the hysteresis factor  $\kappa_r$  and differ from each other only in scale.

When combining relative quantities (1)–(3), expressions for zero-order dimensionless hysteresis quantities can be obtained [14]. In approximation  $F \approx 1$ , we obtain

$$\frac{B_r H_{\max}}{W_h} = \frac{3}{8}; \quad (8)$$

$$\frac{B_{\max} H_c}{W_h} = \frac{3}{8}; \quad (9)$$

$$\frac{B_{\max} H_c}{B_r H_{\max}} = 1. \quad (10)$$

These expressions connecting the hysteresis and limiting quantities do not include the initial permeability  $\mu_i$ , Rayleigh constant  $\eta$ , and hysteresis factor  $\kappa_r$ , which are characteristic of the Rayleigh range. This circumstance directly indicates their high universality with respect to expressions (1)–(3) obtained for the Rayleigh range.

Relations between the hysteresis losses and different combinations of limiting and hysteresis quantities follow from the expressions (8) and (9) for the zero-order dimensionless hysteresis quantities:

$$W_h = \frac{8B_r H_{\max}}{3}; \quad (11)$$

$$W_h = \frac{8B_{\max} H_c}{3}; \quad (12)$$

$$W_h = \frac{8B_{\max}^2 H_c^2}{3B_r H_{\max}}; \quad (13)$$

$$W_h = \frac{8B_r^2 H_{\max}^2}{3B_{\max} H_c}; \quad (14)$$

$$W_h = \frac{8}{3} \sqrt{B_r B_{\max} H_c H_{\max}}. \quad (15)$$

It was shown in [14, 15] that the relative quantities  $B_r/B_{\max}$ ,  $H_c/H_{\max}$ ,  $W_h/W_{\max}$  are similar to each other not only within the Rayleigh range. The similarity of these quantities covers the whole magnetic field range corresponding to the increase in the magnetic permeability of a substance. Therefore, we expect that expressions for hysteretic losses can be used, at least, within this magnetic field range.

Table 1 shows the measured parameters of minor magnetic hysteresis loops for the nanocrystalline  $\text{Fe}_{72.5}\text{Cu}_1\text{Nb}_2\text{Mo}_{1.5}\text{Si}_{14}\text{B}_9$  alloy. Three right columns give the magnetic permeability  $\mu$ , Rayleigh constant  $\eta$ , and hysteresis factor  $\kappa_r$ , which were calculated using measured values and Eqs. (6) and (16). Note that,

**Table 1.** Parameters of minor magnetic hysteresis loops of the nanocrystalline Fe<sub>72.5</sub>Cu<sub>1</sub>Nb<sub>2</sub>Mo<sub>1.5</sub>Si<sub>14</sub>B<sub>9</sub> alloy

| $H_{max}$ , A/m | $B_{max}$ , T | $B_r$ , T             | $H_c$ , A/m           | $W_h$ , J/m <sup>3</sup> | $\mu$  | $\eta \times 10^{-5}$ ,<br>(A/m) <sup>-1</sup> | $\kappa_r$ |
|-----------------|---------------|-----------------------|-----------------------|--------------------------|--------|--|------------|
| 0.030           | 0.00274       | $3.06 \times 10^{-5}$ | $3.35 \times 10^{-4}$ | $2.45 \times 10^{-6}$    | 72600  | 0.54   | 43.1       |
| 0.055           | 0.00502       | $9.31 \times 10^{-5}$ | 0.00102               | $1.37 \times 10^{-5}$    | 73100  | 0.50   | 25.6       |
| 0.081           | 0.00747       | $1.94 \times 10^{-4}$ | 0.00210               | $4.19 \times 10^{-5}$    | 73500  | 0.47   | 18.3       |
| 0.105           | 0.0099        | $3.17 \times 10^{-4}$ | 0.00336               | $8.87 \times 10^{-5}$    | 75100  | 0.46   | 14.6       |
| 0.244           | 0.0244        | 0.00202               | 0.0199                | 0.00124                  | 79500  | 0.51   | 5.6        |
| 0.335           | 0.0465        | 0.00976               | 0.0719                | 0.0086                   | 110300 | 1.36   | 1.5        |
| 0.395           | 0.0629        | 0.0175                | 0.110                 | 0.0183                   | 126700 | 1.77   | 1.0        |
| 0.50            | 0.119         | 0.0589                | 0.254                 | 0.0817                   | 189100 | 3.90   | 0.36       |
| 0.60            | 0.242         | 0.155                 | 0.394                 | 0.275                    | 320700 | 7.58   | 0.15       |
| 0.71            | 0.409         | 0.304                 | 0.469                 | 0.60                     | 458400 | 9.99   | 0.10       |
| 0.84            | 0.522         | 0.403                 | 0.512                 | 0.86                     | 494000 | 8.64   | 0.10       |
| 1.56            | 0.769         | 0.583                 | 0.608                 | 1.60                     | 392100 | 2.52   | 0.18       |
| 5.0             | 1.02          | 0.709                 | 0.68                  | 2.67                     | 161800 | 1.27   | 1.1        |

within the Rayleigh range, the Rayleigh constant and hysteresis factor are  $\eta = 0.50 \times 10^{-5}$  (A/m)<sup>-1</sup> and  $\kappa_r > 1$ , respectively.

Figure 1 shows the dependences of measured (see Table 1) and calculated (by Eqs. (11)–(15)) hysteresis losses  $W_h$  on the maximum magnetic field  $H_{max}$ , which are plotted on logarithmic coordinates. We can see that the curves coincide not only within the Rayleigh range but also within the whole range corresponding to the increase in the magnetic permeability. The coincidence is observed up to the magnetic field  $H_{max} = 0.8$  A/m, which corresponds to the maximum magnetic permeability of the nanocrystalline Fe<sub>72.5</sub>Cu<sub>1</sub>Nb<sub>2</sub>Mo<sub>1.5</sub>Si<sub>14</sub>B<sub>9</sub> alloy. The errors of determination of the hysteresis losses are not given in the plot since, on logarithmic coordinates, the error values do not exceed the symbol size. In the range corresponding to approaching magnetic saturation (after the magnetization curve bend), the calculated and measured curves of hysteresis losses diverge. Note that Eqs. (12) and (15) allow us to obtain a closer agreement with the experimental results over the whole measurement range.

The curves plotted on logarithmic coordinates (Fig. 1) indicate two linear portions, which can be represented in the form of power function  $Y = rX^s$  with the unchanged power index  $s$ . Within the Rayleigh range, the power index  $s$  for the dependence of hysteretic losses  $W_h$  on the maximum magnetic field  $H_{max}$  is equal to 2.97, which corresponds to the power index in the expression obtained from the Rayleigh equations [16],

$$W_h = \frac{4\eta\mu_0 H_{max}^3}{3}. \quad (16)$$

In the range corresponding to the maximum increase in the permeability, the power index increases to 5.94.

Figure 2 shows the dependences of measured and calculated (by Eqs. (11)–(15)) hysteretic losses on the maximum magnetic induction, which are plotted on logarithmic coordinates. The measured and calculated curves also coincide not only within the Rayleigh range but also over the whole range corresponding to the increase in the magnetic permeability. In the low magnetic field,  $s = 2.88$  and the power index is close to 3, which is obtained by Eq. (16) in the low-magnetic field approximation  $B_{max} \approx \mu_r\mu_0 H_{max}$ . Outside the Rayleigh range, the dependence of the measured

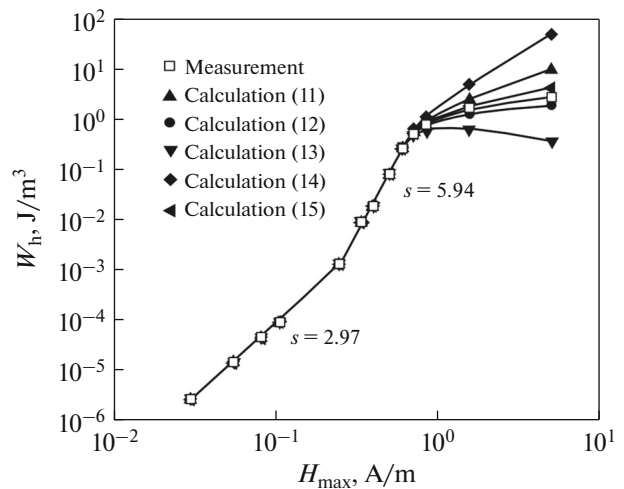


**Fig. 1.** Dependences of the measured and calculated (by Eqs. (11)–(15)) hysteresis losses  $W_h$  on the maximum magnetic field  $H_{max}$ .

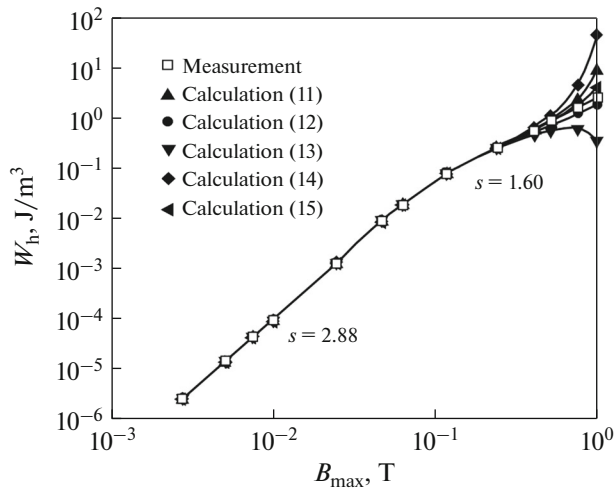


**Fig. 2.** Dependences of the measured and calculated (by Eqs. (11)–(15)) hysteresis losses  $W_h$  on the maximum magnetic induction  $B_{\max}$ .

hysteretic losses is described adequately by power function with the power index equal to 1.60. Such a value was also obtained by Steinmetz [4] for iron with isotropic magnetic properties.

Figure 3 shows the dependences of measured and calculated (by Eqs. (11)–(15)) hysteresis losses on the remanence  $B_r$ , which are plotted on logarithmic coordinates. The adequate agreement between the measured and calculated curves is observed within the whole range of magnetic field, which corresponds to the increase in the magnetic permeability.

Using the Rayleigh equations, we can find the dependence of the remanence on the magnetic field [16]

$$B_r = \frac{1}{2} \eta \mu_0 H_{\max}^2, \quad (17)$$

whereas the expression connecting the hysteresis losses and remanence within the Rayleigh range can be derived using Eqs. (16) and (17):

$$W_h = \frac{8\sqrt{2}}{3(\eta\mu_0)^{0.5}} B_r^{1.5}. \quad (18)$$

Therefore, within the Rayleigh range, the power function connecting the hysteresis losses and remanence should have the power index  $s = 1.5$ . This value almost coincides with the experimental value 1.49 in Fig. 3. Outside the Rayleigh range, the power index decreases to 1.24. Note that, in [9, 10, 17, 18] for the analogous dependences for different ferromagnetic materials, the power index equal to 1.35 was obtained over the whole range of the measured values of remanence  $B_r$ . The close value,  $s = 1.33$ , can be obtained by linear extrapolation of our results over the whole range of the measured values of remanence.

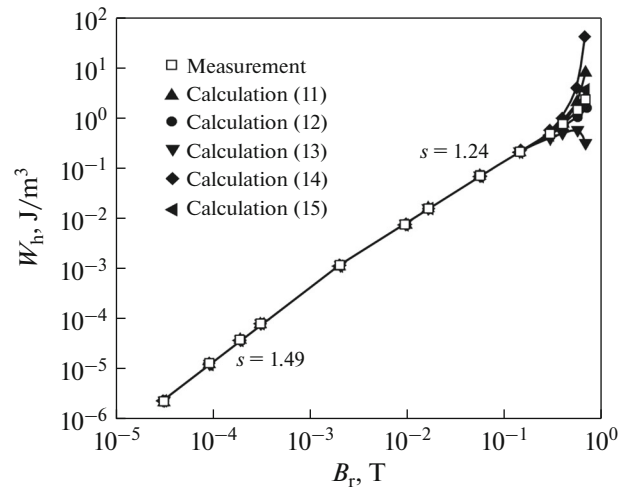


**Fig. 3.** Dependences of the measured and calculated (by Eqs. (11)–(15)) hysteresis losses  $W_h$  on the remanence  $B_r$ .

Within the Rayleigh range, for the condition  $\mu_i \gg \eta H_{\max}$ , the squared relationship between the coercive force and magnetic field can be obtained from Eq. (2):

$$H_c = \frac{\eta H_{\max}^2}{2\mu_i}, \quad (19)$$

whereas, using Eqs. (16) and (19), the relationship connecting the hysteresis losses and coercive force within the Rayleigh range can be obtained:

$$W_h = \frac{8\sqrt{2}\mu_0\mu_i^{1.5}}{3\eta^{0.5}} H_c^{1.5}. \quad (20)$$

The power index  $s = 1.5$  adequately agrees with the experimental value  $s = 1.53$  (Fig. 4). We can see that the measured and calculated dependences of the hysteresis losses on the coercive force coincide over the whole magnetic field range corresponding to the increase in the magnetic permeability.

Equations (8) and (10) for the zero-order dimensionless quantities allow us also to derive relationships connecting the remanence with different combinations of limiting and hysteresis magnitudes:

$$B_r = \frac{B_{\max} H_c}{H_{\max}}; \quad (21)$$

$$B_r = \frac{3W_h}{8H_{\max}}; \quad (22)$$

$$B_r = \frac{8B_{\max}^2 H_c^2}{3W_h H_{\max}}; \quad (23)$$

$$B_r = \sqrt{\frac{3W_h B_{\max} H_c}{8H_{\max}^2}}; \quad (24)$$

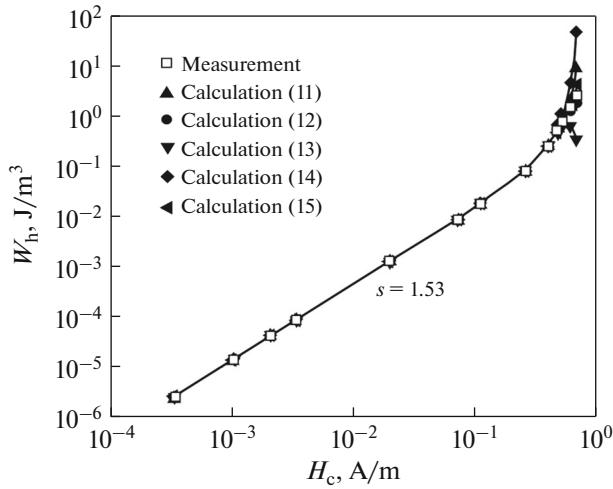


Fig. 4. Dependences of the measured and calculated (by Eqs. (11)–(15)) hysteresis losses  $W_h$  on the coercive force  $H_c$ .

$$B_r = \frac{9W_h^2}{64B_{\max}H_{\max}H_c}. \quad (25)$$

Figure 5 shows the dependences of the measured and calculated (by Eqs. (21)–(25)) values of remanence  $B_r$  on the maximum magnetic field  $H_{\max}$ , which are plotted on logarithmic coordinates.

Similarly to the curves for the hysteresis losses, curves for the remanence coincide not only within the Rayleigh range but also over the whole magnetic field range corresponding to the increase in the magnetic permeability. The power index for the Rayleigh range, which was found from the linear dependence (plotted on logarithmic coordinates) of the remanence  $B_r$  on the maximum magnetic field  $H_{\max}$ , is equal to 1.99 and almost coincides with the power index in Eq. (17). In the range of maximum permeability, the power index increases to 5.94.

Similarly, the relationships for the coercive force can be derived from Eqs. (9) and (10):

$$H_c = \frac{B_r H_{\max}}{B_{\max}}; \quad (26)$$

$$H_c = \frac{3W_h}{8B_{\max}}; \quad (27)$$

$$H_c = \sqrt{\frac{3W_h B_r H_{\max}}{8B_{\max}^2}}; \quad (28)$$

$$H_c = \frac{8B_r^2 H_{\max}^2}{W_h B_{\max}}; \quad (29)$$

$$H_c = \frac{9W_h^2}{64B_r B_{\max} H_{\max}}. \quad (30)$$

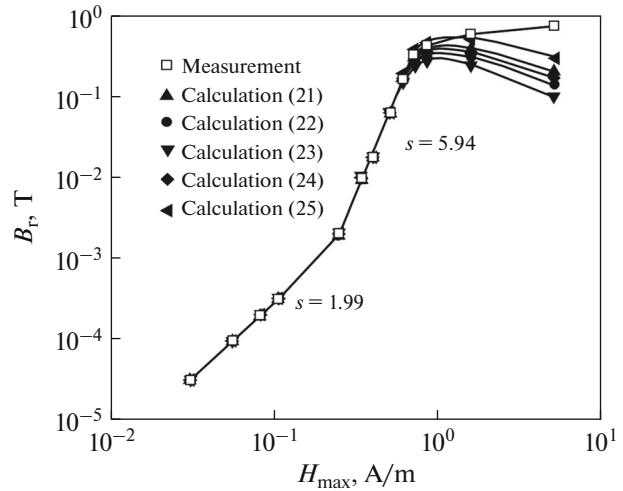


Fig. 5. Dependences of the measured and calculated (by Eqs. (21)–(25)) remanence  $B_r$  on the maximum magnetic field  $H_{\max}$ .

Figure 6 shows the dependences of the measured and calculated (by Eqs. (26)–(30)) values of coercive force  $H_c$  on the magnetic field  $H_{\max}$ , which are plotted on logarithmic coordinates. Similarly, the coercive force curves coincide not only within the Rayleigh range but also over the whole magnetic field range corresponding to the increase in the magnetic permeability. The power index for the Rayleigh range, which was determined from the linear dependence (plotted on logarithmic coordinates) of the coercive force  $H_c$  on the maximum magnetic field  $H_{\max}$ , is equal to 1.94 and close to the power index in Eq. (19). Within the range corresponding to the maximum magnetic permeability, the power index increases to 3.52.

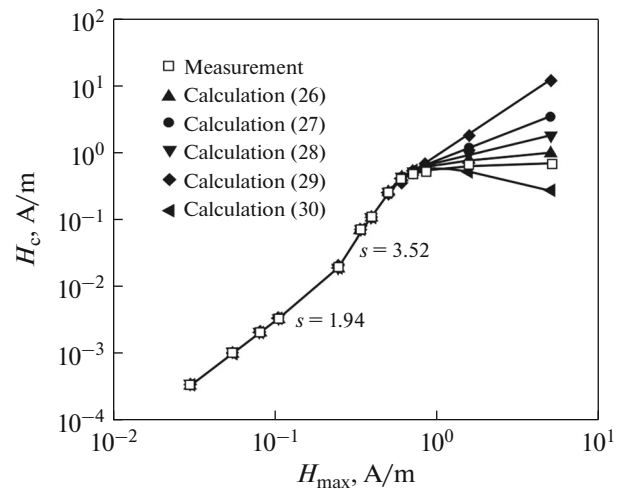


Fig. 6. Dependences of the measured and calculated (by Eqs. (26)–(30)) coercive force  $H_c$  on the maximum magnetic field  $H_{\max}$ .

The obtained results confirm that the hysteresis quantities, namely, the coercive force  $H_c$ , remanence  $B_r$ , and hysteresis losses  $W_h$  are interrelated and this interrelation can be presented in analytical form. The possibility of such an interrelation follows from the similarity of dimensionless hysteresis quantities within the magnetic field range corresponding to the increase in magnetic permeability.

According to the traditional concept [16], the origin of hysteresis within the Rayleigh range is related to irreversible jump-like motion of domain walls and their fragments, which results from the overcoming of local potential barriers. The magnetization reversal processes outside the Rayleigh range differ in the substantial increase in the permeability. This fact can indicate involving a new mechanism in the magnetization reversal process. However, the use of relationships obtained from the Rayleigh equations indicates that the relationships ensure the adequate agreement with the experimental results also for the range corresponding to the maximum increase in the permeability. This indicates the fact that, within the Rayleigh range and range corresponding to the maximum increase in the permeability, similar hysteresis processes, namely, the jump-like motion of domain walls, occur. Only within the range corresponding to the maximum increase in the permeability, the magnetization reversal is realized via irreversible domain-wall jump avalanche rather than single jumps.

At the same time, it is known [19] that, after heat treatment, the nanocrystalline alloy is characterized by low value of magnetic anisotropy constant and is almost magnetically isotropic. For the isotropic alloy, the initial permeability due to the uniform magnetization rotation can be estimated by the expression [16]

$$\mu_{ir} = \frac{\mu_0 M_s^2}{3K}. \quad (31)$$

When substituting the values  $M_s = 10^6$  A/m and  $K = 10$  J/m<sup>3</sup>, we obtain  $\mu_{ir} = 42000$  that largely explains the observed magnetic permeability values. Thus, because of the low magnetic anisotropy constant of the nanocrystalline alloy, the magnetization rotation mechanism can be realized already in the low magnetic field.

In the case of uniform rotation, the hysteresis is absent. However, according to data on the observed domain structure [20, 21], the magnetization rotation in the nanocrystalline alloy with the low magnetic anisotropy constant is nonuniform. The nonuniform rotation is accompanied by substantial transformation of domain structure, in particular, via the motion and the formation and disappearance of domain walls. Thus, the magnetic hysteresis, which results from the nonuniform magnetization rotation, can also be related to the domain wall motion.

## CONCLUSIONS

Relationships between the parameters of static magnetic hysteresis loops, namely, between the hysteresis losses, coercive force, and remanence, were obtained in this study. The interrelation of the hysteresis quantities follows from the similarity of variations of dimensionless hysteresis quantities with increasing magnetic field. The similarity is observed up to the magnetic field corresponding to the maximum magnetic permeability. The similarity was checked experimentally for the soft magnetic nanocrystalline Fe<sub>72.5</sub>Cu<sub>1</sub>Nb<sub>2</sub>Mo<sub>1.5</sub>Si<sub>14</sub>B<sub>9</sub> alloy. We have shown that, in the magnetic field range corresponding to the increase in the magnetic permeability, any hysteresis quantity for the minor loop can be calculated using experimental values of the other hysteresis quantities and limiting values of the magnetic induction  $B_{max}$  and magnetic field strength  $H_{max}$ . The approximation of experimental dependences of hysteresis quantities in low magnetic fields with a power function allows us to obtain the adequate agreement of the power indexes with those calculated by Rayleigh equations.

## ACKNOWLEDGMENTS

This work was supported by the Ministry of Education and Science of the Russian Federation in the framework of state tasks no. 3.6121.2017/8.9 and no. 4.9541.2017/8.9.

## REFERENCES

1. R. Hilzinger and W. Rodewald, *Magnetic Materials. Fundamentals, Products, Properties, Applications* (Wiley, 2013).
2. Yu. N. Starodubtsev, *Magnetically Soft Materials. Encyclopedic Dictionary-Handbook* (Tekhnosfera, Moscow, 2011) [in Russian].
3. G. Bertotti, *Hysteresis in Magnetism* (Academic, San Diego, 1998).
4. C. P. Steinmetz, "On the relationship between magnetic losses and domain structure law of hysteresis," Proc. IEEE **72**, 197–221 (1989), preprinted from the Amer. Inst. Electr. Eng. Trans. **9**, 3–64 (1892).
5. Y. Sakaki and T. Matsuoka, "Hysteresis losses in Mn–Zn ferrite cores," IEEE Trans. Magn. **22**, 623–625 (1986).
6. Yu. N. Starodubtsev and V. A. Kataev, "On the relationship of magnetic losses with the nature of the behavior of the domain structure in silicon-iron single crystals," Fiz. Met. Metalloved. **64**, 1076–1083 (1987).
7. Y.-L. He and G. C. Wang, "Observation of dynamic scaling of magnetic hysteresis in ultrathin ferromagnetic Fe/Au (001) films," Phys. Rev. Lett. **70**, 2336–2339 (1993).
8. P. Kollár, V. Vojtek, Z. Birčáková, J. Füzér, M. Fáberová, and R. Bureš, "Steinmetz law in iron-phenolformaldehyde resin soft magnetic composites," J. Magn. Magn. Mater. **353**, 65–70 (2014).

9. S. Kobayashi, T. Fujiwara, S. Takahashi, H. Kikuchi, Y. Kamada, K. Ara, and T. Shishido, "The effect of temperature on laws of hysteresis loops in nickel single crystals with compressive deformation," *Philos. Mag.* **89**, 651–664 (2009).
10. S. Kobayashi, S. Takahashi, T. Shishido, Y. Kamada, and H. Kikuchi, "Low-field magnetic characterization of ferromagnets using a minor-loop scaling law," *J. Appl. Phys.* **107**, 023908 (2010).
11. R. Tanaka, M. Sasaki, and T. Shirane, "Temperature dependence of minor hysteresis loop NiZn ferrite measured by lock-in amplifier," *IEEE Trans. Magn.* **51**, No. 6100304, (2010).
12. S. Dutz, R. Hergt, J. Mürbe, R. Müller, M. Zeisberger, W. Andrä, J. Töpfer, and M. E. Bellemann, "Hysteresis losses of magnetic nanoparticle powders in the single domain size range," *J. Magn. Magn. Mater* **308**, 305–312 (2007).
13. V. S. Tsepelev, Yu. N. Starodubtsev, and N. P. Tsepel'eva, "Hysteresis properties of the amorphous high permeability  $\text{Co}_{66}\text{Fe}_3\text{Cr}_3\text{Si}_{15}\text{B}_{13}$  alloy," *AIP Adv.* **8**, No. 047707, (2018).
14. Yu. N. Starodubtsev, V. A. Kataev, and V. S. Tsepelev, "Dimensionless quantities of hysteresis loops," *J. Magn. Magn. Mater* **460**, 146–152 (2018).
15. Yu. N. Starodubtsev and V. S. Tsepelev, "Similarity of hysteresis values," *Phys. Met. Metallogr.* **119**, 776–781 (2018).
16. S. Chikazumi, *Physics of Ferromagnetism* (Syokabo, Tokio, 1984; Mir, Moscow, 1987; University Press, Oxford, 1997).
17. S. Takahashi, S. Kobayashi, Y. Kamada, H. Kikuchi, L. Zhang, and K. Ara, "Analysis of minor hysteresis loops and dislocations in Fe," *Physica B* **372**, 190–193 (2006).
18. S. Kobayashi, S. Takahashi, H. Kikuchi, and Y. Kamada, "Domain-wall pinning in Er and Dy studied by minor-loop scaling laws," *J. Phys.: Conf. Ser.* **266**, No. 012015, (2011).
19. G. Herzer, "Nanocrystalline Soft Magnetic Alloys," in *Handbook of Magnetic Materials*, vol. 10, Ed. by K. H. J. Buschow (Elsevier, Amsterdam, 1997), pp. 415–462.
20. S. Flohrer, R. Schäfer, C. Polak, and G. Herzer, "Interplay of uniform and random anisotropy in nanocrystalline soft magnetic alloys," *Acta Mater.* **53**, 2937–2942 (2005).
21. R. Schäfer, "The Magnetic Microstructure of Nanostructured Materials," in *Nanoscale Magnetic Materials and Applications*, Ed. by J. P. Liu, E. Fullerton, O. Gutfleisch, and D. J. Sellmyer (Springer, Dordrecht, 2009) pp. 275–307.

*Translated by N. Kolchugina*